AMERICAN SOCIETY FOR MICROBIOLOGY | Antimicrobial Agents and Chemotherapy

Sustained Nitric Oxide-Releasing Nanoparticles Induce Cell Death in *Candida albicans* Yeast and Hyphal Cells, Preventing Biofilm Formation *In Vitro* and in a Rodent Central Venous Catheter Model

Mohammed S. Ahmadi,[a] Hiu Ham Lee,[a] David A. Sanchez,[b] Adam J. Friedman,[c] Moses T. Tar,[d] Kelvin P. Davies,[d] Joshua D. Nosanchuk,[e,f] Luis R. Martinez[a]

Department of Biomedical Sciences, NYIT College of Osteopathic Medicine, New York Institute of Technology, Old Westbury, New York, USA[a]; Howard University College of Medicine, Washington, DC, USA[b]; Department of Dermatology, George Washington University School of Medicine and Health Sciences, Washington, DC, USA[c]; Departments of Urology,[d] Medicine (Division of Infectious Diseases),[e] and Microbiology and Immunology,[f] Albert Einstein College of Medicine, Bronx, New York, USA

***Candida albicans* is a leading nosocomial pathogen. Today, candidal biofilms are a significant cause of catheter infections, and such infections are becoming increasingly responsible for the failure of medical-implanted devices. *C. albicans* forms biofilms in which fungal cells are encased in an autoproduced extracellular polysaccharide matrix. Consequently, the enclosed fungi are protected from antimicrobial agents and host cells, providing a unique niche conducive to robust microbial growth and a harbor for recurring infections. Here we demonstrate that a recently developed platform comprised of nanoparticles that release therapeutic levels of nitric oxide (NO-np) inhibits candidal biofilm formation, destroys the extracellular polysaccharide matrices of mature fungal biofilms, and hinders biofilm development on surface biomaterials such as the lumen of catheters. We found NO-np to decrease both the metabolic activity of biofilms and the cell viability of *C. albicans in vitro* and *in vivo*. Furthermore, flow cytometric analysis found NO-np to induce apoptosis in biofilm yeast cells *in vitro*. Moreover, NO-np behave synergistically when used in combination with established antifungal drug therapies. Here we propose NO-np as a novel treatment modality, especially in combination with standard antifungals, for the prevention and/or remediation of fungal biofilms on central venous catheters and other medical devices.**

Many clinical manifestations are attributed to the human commensal fungus *Candida albicans*, especially to its ability to form biofilms on implanted medical devices (1). Biomaterials commonly used in clinical practice (e.g., central venous catheters [CVCs], dentures, and heart valves) are fertile grounds for *C. albicans* colonization and biofilm formation, thus establishing the onset and progression of disease (2, 3). Particularly, CVCs are a high risk for *C. albicans* biofilm-related infection by nature of direct contact with patient's bloodstream; it is therefore no surprise that this organism is the 4th leading cause of bloodstream infections in the United States (4, 5). Forty percent of patients with *C. albicans* biofilm-infected intravenous catheters develop fungemia, resulting in diverse outcomes ranging from focal disease to severe sepsis and death (6). Current guidelines for the treatment of catheter-associated candidemia advocate for line removal to facilitate more rapid clearance of the bloodstream and better prognosis (4). In contrast to removal of peripheral intravenous catheters, removal of larger CVCs is not always feasible, and replacement is expensive and associated with a procedural risk for the patient. The profound economic consequences of *Candida* infections is highlighted by the ~$1.7 billion spent annually on treating candidemia in the United States alone (7) and an estimated cost per infection of ~$34,508 to $56,000 (8, 9). In this scenario, there is a need for novel strategies to combat fungal contamination of prosthetic devices, especially biofilm-related infections that exacerbate morbidity, resulting in high mortality (6).

Mature *C. albicans* biofilms consist of a unique niche for microbial growth, in which the fungus is highly equipped for survival as biofilms contain heterogeneous morphological forms, including yeasts, hyphae, and pseudohyphae, in a precise arrangement encased in an exogenous matrix that consists of carbohydrates and proteins (1). Cells within biofilms show different properties from their planktonic counterparts, such as increased resistance to antimicrobial agents, multiple drug resistance, and tolerance to host defenses. Microbes can disseminate from the self-contained environment of biofilms, leading to persistent infections, especially in individuals with compromised immunity. Dispersed *C. albicans* cells are mostly in the yeast form and display distinct phenotypic properties compared to those of planktonic cells, including enhanced adherence, filamentation, and biofilm formation and increased pathogenicity in a murine model of systemic candidiasis (10). Furthermore, persister *C. albicans* cells have been described, dormant variants of regular fungal cells that form stochastically in microbial populations and are highly tolerant to antifungal drugs (11). Persister cells are an important mechanism of resistance in chronic infections (12), and a mechanism of resistance that has gathered some attention recently in fungal biofilms (11, 13).

To combat the unique impediment represented by *C. albicans* biofilms, we investigated a molecule produced by the innate immune system. Nitric oxide (NO) is a diatomic lipophilic gaseous

Received 2 November 2015 **Returned for modification** 14 November 2015
Accepted 19 January 2016

Accepted manuscript posted online 25 January 2016

Citation Ahmadi MS, Lee HH, Sanchez DA, Friedman AJ, Tar MT, Davies KP, Nosanchuk JD, Martinez LR. 2016. Sustained nitric oxide-releasing nanoparticles induce cell death in *Candida albicans* yeast and hyphal cells, preventing biofilm formation *in vitro* and in a rodent central venous catheter model. Antimicrob Agents Chemother 60:2185–2194. doi:10.1128/AAC.02659-15.

Address correspondence to Luis R. Martinez, lmarti13@nyit.edu.

molecule produced by numerous immune cells as both a cytostatic and cytotoxic broad-spectrum antimicrobial agent (14–16). NO has been shown to be effective against *C. albicans* despite the fungus's inherent (17, 18), inducible NO defense mechanism (19). We have previously demonstrated the efficacy of a platform technology using nitric oxide-releasing nanoparticles (NO-np) (20, 21) against *C. albicans* cutaneous burn infections, which was found to effectively interfere with fungal growth and morphogenesis (18). Therefore, this technology can be potentially used and applied as a tool to combat biofilm-infected medical implants. The simplicity and stability of NO-np for use in sustained delivery of NO make the nanoparticles a very attractive treatment modality.

In this study, we used a CVC *C. albicans* biofilm model (22) to investigate the efficacy of NO-np in preventing and eradicating biofilms. We demonstrated the susceptibility of mature *C. albicans* biofilms grown *in vitro* and on CVCs implanted in Sprague-Dawley rats after treatment with NO-np. Sustained delivery of NO displayed a potent efficacy in inhibiting biofilm formation and killing mature biofilms by *C. albicans* clinical isolates. Moreover, NO-np were more effective than clinically used antifungal drugs for treatment of *C. albicans* biofilms, suggesting that this nanotechnology can be utilized as a therapeutic agent for the prevention and treatment of catheter-associated *C. albicans* biofilm infections.

MATERIALS AND METHODS

Candida albicans. *C. albicans* SC5314 was obtained from Mahmoud Ghannoum (Cleveland, OH). A total of 10 *C. albicans* clinical strains (0435, 0806, 4022, 5161, 5196, 5213, 5518, 6926, 8859, and 9081) isolated from blood at the Montefiore Medical Center (MMC), Bronx, NY, were included in this study. All samples were obtained with the written consent of all patients according to the practices and standards of the institutional review boards at the Albert Einstein College of Medicine (Einstein) and MMC. In addition, all studies were conducted according to the Declaration of Helsinki principles. All the strains were stored at −80°C in yeast extract, peptone, and dextrose (YPD) broth (Difco, Becton Dickinson [BD]) with 50% glycerol until use. Test organisms were grown in YPD broth for 24 h at 30°C using a rotary shaker set at 150 rpm.

Synthesis of NO-np. A hydrogel-glass composite was synthesized using a mixture of tetramethyl orthosilicate, polyethylene glycol, chitosan, glucose, and sodium nitrite in a 0.5 mM sodium phosphate buffer (pH 7) as previously described (23). Briefly, the nitrite was reduced to NO within the matrix because of the glass properties of the composite affecting redox reactions initiated with thermally generated electrons from glucose. After redox reaction, the ingredients were combined and dried using a lyophilizer, resulting in a fine powder comprising nanoparticles containing NO. Once exposed to an aqueous environment, the hydrogel properties of the composite allow for an opening of the water channels inside the particles, facilitating the release of the trapped NO over extended periods. Nanoparticles lacking NO were also produced to serve as controls.

Amperometric detection of NO release. NO released from the nanoparticles was determined by amperometric detection using the Apollo 4000 nitric oxide detector (World Precision Instruments Ltd.) as previously described (20). The system uses a composite graphite NO-sensing element coated with an NO-selective membrane coupled with a reference electrode that senses NO levels down to the subnanomolar range (24). Due to its NO specificity, rapid response time, and detection limits (1 nM minimum), the ISO-NOP sensor (World Precision Instruments Ltd.) was used. Briefly, argon-degassed 0.05 M phosphate buffer was saturated with NO gas, resulting in a 1.9 mM solution of NO. The ISO-NOP sensor was equilibrated with 20 ml of 0.05 M phosphate buffer under stirring conditions. Aliquots of a saturated NO solution were added and a linear calibration curve was generated from the resulting data. Measurements of NO release from the np were derived using this method, except that 100 mg of NO-np was added. Data were collected over time and correlated against the calibration curve, allowing for reproducible measurements of NO concentration in solution over time. The observed trace indicates a relatively stable rate of NO release, with only a slight initial peak (5.64×10^{-6} μg/ml, or 18.75 nM) at 70 min. A steady-state level (3.76×10^{-6} μg/ml, or 12.5 nM) is achieved after 6 h with continuous release occurring over ~24 h.

Biofilm formation. Fungal cells were collected by centrifugation, washed twice with phosphate-buffered saline (PBS), counted using a hemacytometer, and suspended at 10^7 cells/ml in a chemically defined minimal medium (20 mg/ml of thiamine, 30 mM glucose, 26 mM glycine, 20 mM $MgSO_4 \cdot 7H_2O$, and 58.8 mM KH_2PO_4) supplemented with 5% fetal calf serum (FCS; Atlanta Biologicals). Then, 100 μl of the suspension was added into individual wells of polystyrene 96-well plates (Fisher Scientific) and incubated at 37°C. Biofilms were allowed to develop over a series of time intervals (2, 8, 24, and 48 h). Wells containing biofilms were washed three times with PBS. Cells remaining attached to the surface of the wells were considered viable biofilms. Three wells in the absence of *C. albicans* cells were utilized as controls. All assays were carried out in triplicate.

Susceptibilities of fungal biofilms to NO-np. To evaluate the susceptibilities of fungal biofilms to NO-np, PBS containing 5 mg/ml of np or NO-np in 200 μl was added to each well. This concentration was selected because it was previously shown to be effective against *C. albicans* (18). Mature biofilms containing np or NO-np were agitated for 1 min using a microtiter plate reader to ensure a uniform distribution, followed by incubation at 37°C for 24 h. After incubation, biofilm metabolic activity and cellular viability were quantified. PBS alone (untreated) was used as a control.

Assessing biofilm metabolic activity by XTT reduction assay. A quantitative measurement of *C. albicans* biofilm formation was obtained by assessing the metabolic activity of the attached cells via a 2,3-bis(2-methoxy-4-nitro-5-sulfophenyl)-5-[(phenylamino)carbonyl]-2H-tetrazolium hydroxide (XTT; Sigma) reduction assay as previously described (25).

Measuring biofilm cellular viability by CFU killing assay. The toxicity of NO-np for candidal biofilms was evaluated by a CFU killing assay. After incubation with NO-np, biofilms were scraped from the bottoms of the wells with a sterile 200-μl micropipette tip. A volume of 100 μl of suspension containing dissociated cells was aspirated from the wells, transferred to a microcentrifuge tube with 900 μl of PBS, and sonicated for 1 min. A series of dilutions were then performed, and 100 μl of diluted suspension was plated on Sabouraud dextrose agar (Difco) plates.

Apoptosis assay. Given that *C. albicans* biofilms consist of a combination of yeasts and hyphae surrounded by an exopolymeric matrix (EPM), we assessed whether NO-np induce apoptosis in fungal cells impairing their viability. Apoptotic yeasts or hyphae were analyzed by flow cytometry or fluorescence microscopy, respectively, using an annexin V-fluorescein isothiocyanate (FITC) and propidium iodide (PI) kit (BD).

(i) Flow cytometry. Yeasts suspended at a density of 10^6 cells in PBS were first treated with np or NO-np for 4 h at 37°C and compared to untreated fungal cells. After treatment, fungal cells were washed twice with cold PBS and resuspended in binding buffer. Five microliters of annexin V-FITC and PI were added to cells. Each suspension was gently vortexed and incubated for 15 min at room temperature (RT; 25°C) in the dark. Then, 400 μl of binding buffer was added to each tube and samples were analyzed by flow cytometry within 1 h using a BD Accuri C6 flow cytometer. The percentage of cells positive for PI (red) and/or annexin V-FITC (green) was determined using the FCS express software.

(ii) Fluorescence microscopy. The apoptotic effect of NO-np on the *C. albicans* filamentous form was assessed using fluorescence microscopy. Briefly, 10^6 yeasts were grown in 2 ml of minimal medium supplemented with 5% FCS on a poly-L-lysine-coated coverslip bottom of MatTek

plates. FCS was used because it promotes hyphal formation by *C. albicans*. Plates were incubated for 4 h at 37°C and 5% CO_2. After hyphal formation, plates were washed three times with PBS, and 2 ml of medium supplemented with FCS with either NO-np or np (5 mg/ml) was added to each plate. Then, plates were incubated for 4 h at 37°C and 5% CO_2. Controls included plates containing untreated candidal hyphae. For fluorescence studies, fungal cells were washed three times with cold PBS and resuspended in binding buffer. Ten microliters of annexin V-FITC (green) and PI (red) was added to hyphae and incubated for 1 h at RT (25°C) in the dark. Then, 2 ml of binding buffer was added to each plate and the plates were viewed using an Axiovert 40 CFL inverted microscope (Carl Zeiss). Images were captured with an AxioCam MrC digital camera using Zen 2011 digital imaging software.

***C. albicans* CVC biofilm model.** A *C. albicans* central venous catheter (CVC) biofilm model was used for *in vivo* experiments, as described elsewhere (22, 26). All animal studies were conducted according to the experimental practices and standards approved by the Institutional Animal Care and Use Committee at Einstein. Briefly, female Sprague-Dawley rats weighing 400 g (Charles Rivers) were anesthetized, and the right external jugular was exposed. A longitudinal incision was made in the vein wall, and a sterile, heparinized (100 U/ml) polyethylene catheter (PE 100 [inner diameter, 0.76 mm; outer diameter, 1.52 mm]; BD) was inserted at a site above the right atrium (~2 cm) and secured with 3-0 silk ties. The proximal end of the catheter was tunneled subcutaneously and secured on the subscapular skin by means of a button secured with a 2-0 Ti-Cron suture. The wound was closed with staples (Ethicon Endo-Surgery). After surgery, an inoculum of 10^6 *C. albicans* cells/ml washed and suspended in PBS was instilled in the catheter lumen. Twenty-four hours later, a single dose of 5 mg/ml of np or NO-np was instilled by injection in the catheter lumen ("catheter lock therapy"). Finally, catheters were collected 48 h after infection, longitudinally cut and transected lengthwise (5 pieces of 5-mm catheter per animal; 5 animals per group), transferred to a microcentrifuge tube containing 2 ml of PBS, and sonicated for 1 min to detach adherent cells. Serial dilutions of the cell suspensions were performed and quantified by the CFU killing assay. This experiment was performed once.

Imaging of fungal biofilms. (i) Light microscopy. Examinations of the mature *C. albicans* biofilms formed in microtiter plates were performed by light microscopy with an Axiovert 40 CFL inverted microscope and photographed with an AxioCam MrC digital camera using Zen 2011 digital imaging software.

(ii) Confocal-like microscopy. Mature *C. albicans* biofilms were incubated for 45 min at 37°C in 75 μl of PBS containing the fluorescent stains FUN-1 (10 μM) and concanavalin A-Alexa Fluor 488 conjugate (ConA; 25 μM) (Molecular Probes). FUN-1 (excitation wavelength, 470 nm; emission wavelength, 590 nm) is converted to orange-red cylindrical intravacuolar structures by metabolically active cells, while ConA (excitation wavelength, 488 nm; emission wavelength, 505 nm) binds to the glucose and the mannose residues of cell wall polysaccharides and fluoresces green. Microscopic examinations of the biofilms formed in microtiter plates were performed with an Axiovert 200 M inverted microscope (Carl Zeiss). A 40× objective (numerical aperture, 0.6) was used. Depth measurements across the width of the device were taken at regular intervals. To determine the structure of the biofilms, a series of horizontal (x-y) optical sections with a thickness of 1.175 μm were taken throughout the full length of the biofilm. Images of green and red fluorescence were recorded simultaneously by confocal microscopy using a multichannel mode. Z-stack images and measurements were corrected utilizing Axio Vision 4.4 software in the deconvolution mode.

(iii) SEM. To assess biofilm formation *in vivo*, scanning electron microscopy (SEM) was used to examine the catheters of untreated and NO-np-treated animals. The catheters were transected lengthwise, fixed overnight (4% formaldehyde and 1% glutaraldehyde in PBS), washed for 5 min in PBS, and placed in 1% osmium tetroxide for 30 min. After a series of alcohol washes, the samples were critical-point dried (Samdri-790; Tousimis), mounted, gold coated (Desk-1; Denton Vacuum, Inc.), and viewed in a JEOL JSM-6400 scanning electron microscope in high-vacuum mode at 10 kV.

NO-np and antifungal drug susceptibilities. The susceptibilities of the *C. albicans* biofilms to commonly prescribed antifungal drugs (fluconazole and voriconazole; Pfizer) and NO-np were determined and compared by two independent methods (27). First, the XTT reduction assay was used to measure the diminution in metabolic activity (50% reduction in metabolic activity [RMA]) for biofilms. Second, cell survival in the biofilm suspension was evaluated by the CFU killing assay.

Combination therapy susceptibility assays. Each well with mature fungal biofilms was exposed to 200 μl of a solution containing combinations of either NO-np or np (concentrations of 0.08 to 5 mg/ml) and fluconazole or voriconazole (concentrations of 0.125 to 128 μg/ml). Biofilms treated with combination therapy were incubated for 24 h. The XTT reduction assay was used to determine the metabolic activity of the biofilms.

Synergy testing. The fractional inhibitory concentration index (FICI) was determined using the XTT reduction assay. The FICI was calculated as the sum of the FICs of the antimicrobials. The FIC of an antimicrobial was determined by establishing the MIC of the antimicrobial (A or B) in the combination (MIC^{comb}) divided by the MIC of the antimicrobial acting alone (MIC^{alone}). The formula used to calculate the FICI is as follows: $FICI = FIC_A + FIC_B = {MIC_A}^{comb}/{MIC_A}^{alone} + {MIC_B}^{comb}/{MIC_B}^{alone}$. An FICI of ≤0.5 indicates synergy, an FICI of >0.5 to 4 shows an additive or indifferent effect, and an FICI of >4 reflects an antagonistic interaction.

Statistical analysis. Statistical analyses were obtained utilizing GraphPad Prism 6.0 (GraphPad Software, La Jolla, CA) software. *P* values were calculated by analysis of variance (ANOVA) and were adjusted by use of the Bonferroni correction. *P* values of <0.05 were considered significant.

RESULTS

NO-np impede *Candida albicans* biofilm formation *in vitro*. The kinetics of biofilm formation by 10 *C. albicans* clinical isolates and an ATCC *C. albicans* SC5314 strain on polystyrene microtiter plates in absence or presence of np or NO-np was studied for 48 h using the colorimetric XTT reduction assay. On average, untreated and np-treated *C. albicans* strains displayed similar biofilm formations even though there was a significant increase in metabolic activity at 8 h for the untreated fungal strains compared to np-treated isolates ($P < 0.05$) (Fig. 1A). Control biofilms were metabolically active during the early and intermediate stages that included the adhesion period (2 to 4 h) and microcolony formation (8 to 12 h). In contrast, fungal strains treated with NO-np evinced significantly less adherence of cells on the plastic substrate than control groups as early as 4 h and 8 h for untreated ($P < 0.05$) and np-treated ($P < 0.001$) strains, respectively (Fig. 1A). Consistent with the XTT reduction assay, bright-field images of *C. albicans* SC5314 biofilm formation kinetics revealed that during the adhesion period (4 h), the candidal cells of control groups became firmly attached to the plastic surface of the microtiter plate in a monolayer arrangement (Fig. 1B). The fungal cells adherent to the plastic support consisted of growing cells, as indicated by the presence of many budding cells (Fig. 1B). Conversely, NO-np-treated wells showed a noticeably reduced number of single and spaced cells attached to the plastic surface (Fig. 1B). At the intermediate stage (8 h), the fungal population had increased significantly and consisted of yeast cells and pseudohyphae spread uniformly throughout the plastic support forming microcolonies (Fig. 1B). As observed in the metabolic assay (Fig. 1A), accumulation of cellular mass was more evident in the untreated fungi relative to the np group (Fig. 1B). At this stage, *C. albicans* cells incubated with NO-np demonstrated spread microcolonies with obvious re-

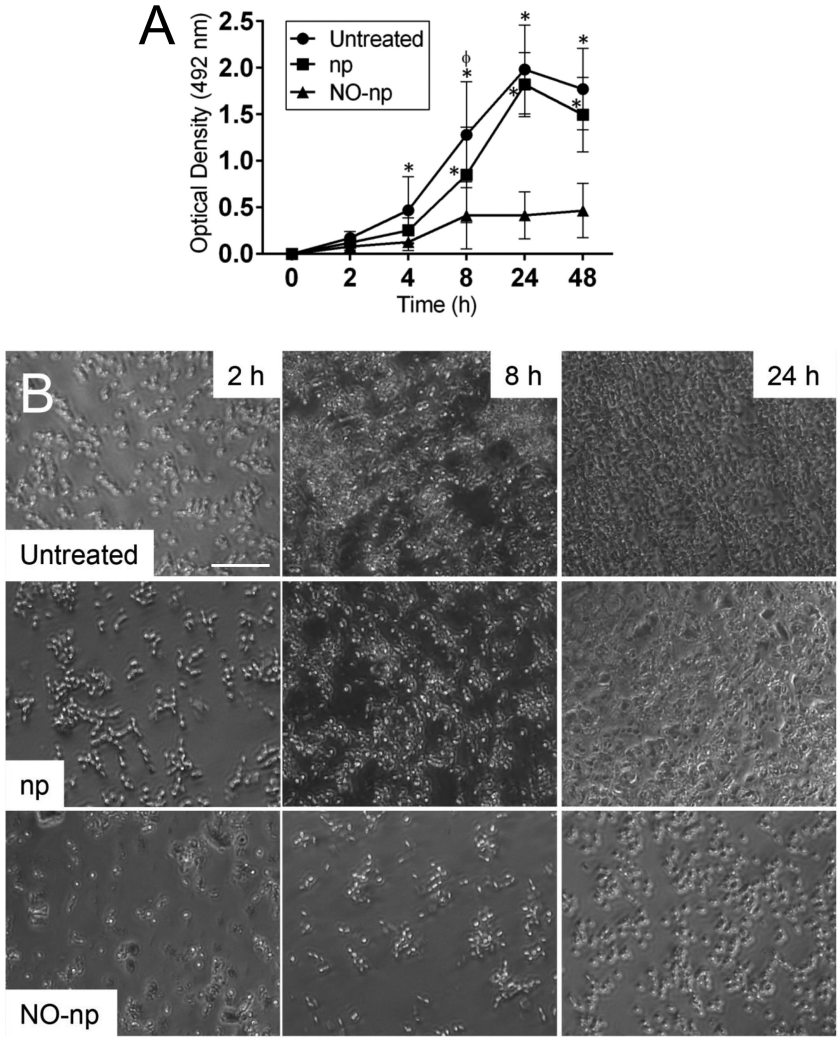

FIG 1 NO-np inhibit biofilm formation by *Candida albicans* clinical isolates. (A) Kinetics of *C. albicans* biofilm formation in polystyrene microtiter plates grown in the absence (untreated) and presence of 5 mg/ml of nanoparticles alone (np) or nitric oxide-releasing nanoparticles (NO-np), as determined by the XTT reduction assay. Each symbol represents the average value ($n = 11$ strains per time point), and error bars indicate standard deviations (SDs). *P* value significance ($P < 0.05$) was calculated by analysis of variance (ANOVA) and adjusted by use of the Bonferroni correction. * and ϕ, significantly higher optical densities (OD) than for NO-np and np groups, respectively. (B) Representative light microscopy images of untreated, np-treated, or NO-np-treated *C. albicans* SC5314 strain biofilms grown on microtiter plates for 2, 8, and 24 h. The pictures were taken at a magnification of ×20. Scale bar, 10 μm. All experiments were performed twice, with similar results obtained each time.

tarded growth (Fig. 1B). During the maturation stage (24 h), the microarchitecture of *C. albicans* biofilms grown in the absence of NO became more complex due to an increasing amount of extracellular material surrounding the cells and producing compact structures that tenaciously adhered to the plastic support (Fig. 1B). However, NO-np-treated cells evidenced delayed biofilm synthesis (Fig. 1B).

Susceptibility of mature *C.* albicans biofilms to NO-np *in vitro*. Forty-eight-hour mature biofilms formed by 11 *C. albicans* strains on polystyrene microtiter plates and treated for 24 h with NO-np showed a significant reduction in metabolic activity when viability was measured by the XTT reduction assay (Fig. 2A). Fungal biofilms grown in the absence of NO demonstrated considerably higher metabolic activity than those biofilms treated with the NO-np ($P < 0.05$, untreated, and $P < 0.001$, np treated). To confirm the results obtained by the XTT reduction assay, the viability of cells in the biofilm was further determined by CFU enumeration (Fig. 2B). On average, *C. albicans* biofilms were significantly susceptible to NO-np after 24 h of treatment with 5 mg/ml of NO-np compared to untreated ($P < 0.05$) or np-treated ($P < 0.001$) biofilms. Confocal-like microscopic examination was used to visualize the effects of NO-np on *C. albicans* biofilm structure (Fig. 2C). Regions of red fluorescence (FUN-1) represent metabolically active cells, and the green fluorescence (ConA) indicates glucose and mannose constituents of the extracellular polysaccharide matrix. *C. albicans* biofilms grown in the presence of PBS alone and np showed regions of high and moderate metabolic activity, respectively (Fig. 2C). The thicknesses of the EPM for untreated and np-treated biofilms were 62 and 59 μm, respectively. Biofilms treated with 5 mg/ml of NO-np manifested a decrease in the thickness (40 μm) of the EPM and number of cells (Fig. 2C).

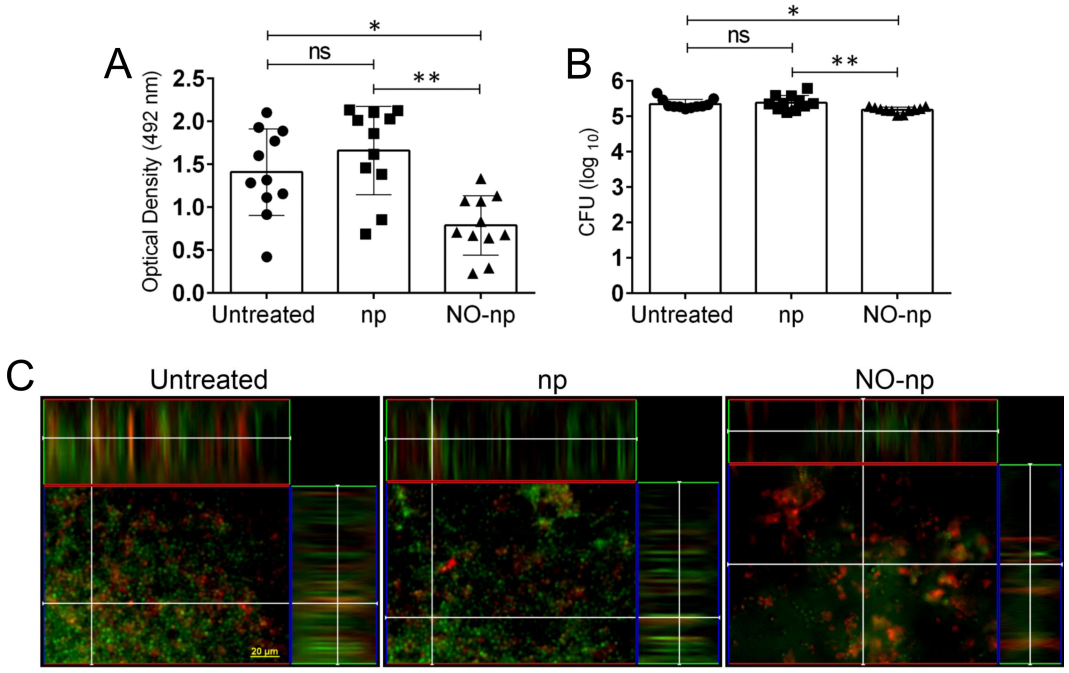

FIG 2 Mature *C. albicans* biofilms are susceptible to NO-np. Forty-eight-hour mature fungal biofilms were exposed to np or NO-np for 24 h, and their metabolic activities and viabilities were compared to those of untreated biofilms using the 2,3-bis(2-methoxy-4-nitro-5-sulfophenyl)-5-[(phenylamino)carbonyl]-2H-tetrazolium hydroxide (XTT) reduction (A) and CFU (B) assays. For panels A and B, each symbol represents a *C. albicans* strain (three OD measurements and CFU plates per strain), bars signify the average ($n = 11$) for each experimental condition, and error bars indicate SDs. *P* value significance (*, $P < 0.05$; **, $P < 0.001$; ns, not significant) was calculated by ANOVA and adjusted by use of the Bonferroni correction. (C) Confocal microscopic examination of untreated, np-treated, or NO-np-treated *C. albicans*. Representative images of biofilms show metabolically active cells (FUN-1 staining, red) embedded in the polysaccharide extracellular material (ConA staining, green); the yellow-brownish areas represent metabolically inactive or nonviable cells. Scale bar, 20 μm. All experiments were performed twice, with similar results obtained each time.

NO-np impact on fungal programmed cell death. Since *C. albicans* biofilms are made up of a mixture of yeasts and hyphae surrounded by an EPM, we investigated whether NO-np facilitate *C. albicans* apoptosis using flow cytometry (Fig. 3A) and fluorescence microscopy (Fig. 3B) to analyze cellular damage in yeast and hyphae, respectively, using annexin V-FITC (green) and PI (red). Viable cells with intact membranes exclude PI, whereas the membranes of dead and damaged cells are permeative to PI. First, flow cytometry of *C. albicans* strain SC5314 validated that untreated yeasts evinced 99.9% viability (Fig. 3A). Similarly, yeast cells treated with np displayed 83.7% viable, 15.2% apoptotic, and 0.5% nonapoptotic dead cells (Fig. 3A). In contrast, NO-np-treated samples gave evidence for a significant early apoptotic population, with only 1.3% viable, 49.2% apoptotic, and 49.2% of the population consisting of nonapoptotic dead cells (Fig. 3A). Due to the fact that flow cytometry is difficult to perform with hyphae, we use fluorescent imaging to determine the role of NO-np in *C. albicans* hyphae (Fig. 3B). Hyphae of untreated *C. albicans* were negative for both annexin V-FITC and PI, suggesting that these fungal cells are alive and not undergoing measurable apoptosis (Fig. 3B). Treatment with np stained hyphal filaments positive for annexin V-FITC and negative for PI, indicating that those threads were undergoing apoptosis (Fig. 3B). Furthermore, NO-np-treated hyphae showcased positive staining for both annexin V-FITC and PI, suggesting that these cells were either in the end stage of apoptosis, were undergoing necrosis, or were already dead (Fig. 3B). Together, our findings demonstrate that NO-np induce cell death by either apoptosis or necrosis in *C. albicans* yeast and hyphal cells.

***In vivo* efficacy of NO-np against fungal biofilms.** We tested the effectiveness of sustained NO-releasing np to inhibit *C. albicans* biofilm formation on catheters *in vitro* and *in vivo*. First and as a proof of principle, we added 5-mm catheters to *C. albicans* SC5314 cultures and incubated them for 24 h at 37°C under shaking conditions. We used CFU counts to assess biofilm formation on catheters in absence and presence of NO. *C. albicans*-colonized catheters treated with NO-np had statistically significantly lower microbial burden than did control catheters ($P < 0.05$, untreated and np) (Fig. 4A). It is possible that the chitosan incorporated into the np may offer some degree of antifungal activity, as demonstrated in the significant difference observed in np-treated catheters relative to controls ($P < 0.05$). Likewise, we used a previously characterized CVC model (22) to mimic device-associated infection to determine whether NO-np would prevent *C. albicans* biofilm formation *in vivo* (Fig. 4B). Our findings revealed that there was a significant difference in fungal burden between catheters treated with NO-np relative to untreated ($P < 0.001$) or np-treated ($P < 0.05$) catheters. Images of the luminal surface of untreated control or NO-np-treated catheters were taken 24 h after inoculation with *C. albicans* (Fig. 4C). *C. albicans* formed extensive biofilms in untreated control catheters, consisting of a network of hyphae (white arrows) and yeast cells (white arrowheads) embedded in EPM (black arrows) (Fig. 4D). Conversely, *C. albicans* biofilms did not form on NO-np-treated catheters

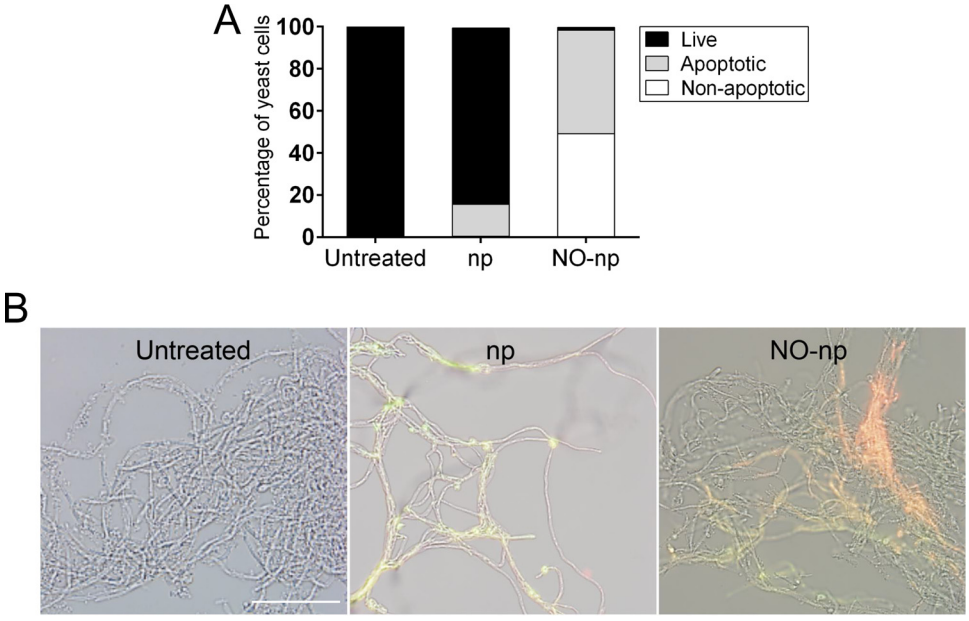

FIG 3 NO-np induces apoptosis and necrosis of *C. albicans* cells. (A) Yeast cells were treated with np or NO-np and compared to untreated fungal cells. Apoptotic cells were analyzed by flow cytometry after being stained with annexin V-FITC together with propidium iodide (PI). The percentages of viable (live) and apoptotic or nonapoptotic dead cells are reported. (B) Fluorescence microscopy images of untreated, np-treated, and NO-np-treated filamentous *C. albicans*. Representative images of fungal hyphae showed viable (no fluorescence), apoptotic (annexin V; green), and dead (PI; red) cells. The pictures were taken at a magnification of ×20. Scale bar, 20 μm. All experiments were performed twice, with similar results obtained each time.

(Fig. 4E). Instead, images showed debris (light gray arrowheads) attached to the catheter's walls (Fig. 4F).

Susceptibility of biofilms formed by *C. albicans* clinical isolates to established antifungals. We determined the susceptibility of the *C. albicans* strains to common antifungal drugs, fluconazole and voriconazole, using Clinical and Laboratory Standards Institute guidelines. The MIC range for fluconazole against 11 fungal strains was 0.25 to 0.5 μg/ml, whereas the range for voriconazole was 0.03 to 0.12 μg/ml (data not shown). However, fungal biofilms are more resistant to antifungal drugs than planktonic cells (27, 28). Therefore, we used two independent methods to demonstrate that the biofilms were more resistant than the planktonic cells to the azoles (Table 1). Similar results were obtained for 50% reduction in metabolic activity (RMA) and survival (RS) for biofilms treated with fluconazole. Both procedures showed that cells within *C. albicans* biofilms were susceptible to 64 μg/ml. In contrast, different results for 50% RMA (64 μg/ml) and RS (32 μg/ml) were obtained for fungal biofilms incubated with voriconazole. Then, we compared the biofilm susceptibility of the azoles to NO-np. RMA and RS quantifications showed that actual lower concentrations of NO (5.64×10^{-6} μg/ml for the initial peak and 3.76×10^{-6} μg/ml for steady state) (20) are required to reduce 50% of the fungal population within biofilms. We did not observe any effect of control np alone on fungal biofilms using RMA and RS protocols (data not shown). We further investigated the efficacy that the combination of either np or NO-np and antifungal therapy has against *C. albicans* SC5314 biofilms. Control np did not affect fungal biofilms in the absence of azole drugs (Fig. 5A to C), whereas a significant reduction in metabolic activity of biofilm-associated cells was shown at concentrations of 0.625 and 1.25 mg/ml of NO-np (Fig. 5B to D). Biofilms treated only with azole drugs showed a considerable drop in metabolic activity at a concentration of 64 μg/ml. *C. albicans* biofilm cells incubated with np and fluconazole showed similar metabolic activity at most np and drug concentrations (Fig. 5A). In contrast, biofilm cells incubated with combinations of ≥0.625 and 1.25 mg/ml of NO-np showed significantly greater susceptibility to 1 and 0.125 μg/ml of fluconazole ($P < 0.001$), respectively (Fig. 5B). Low metabolic activity displayed by biofilms was inversely proportional to increases in the concentration combinations of NO-np and fluconazole in the medium (Fig. 5B). There was no difference in biofilm cell susceptibility when voriconazole was combined with control np (Fig. 5C). When biofilms were treated with NO-np and exposed to voriconazole, *C. albicans* biofilms manifested considerably low levels of cellular metabolism (Fig. 5D). The damaging effect of NO-np was observed at concentrations of >0.03 mg/ml and >0.125 μg/ml of voriconazole (Fig. 5D) ($P < 0.001$). Finally, we calculated FICI to define synergy when NO-np and azole drugs were combined for treatment of *C. albicans* biofilms. The mean FICIs for combination of fluconazole or voriconazole and NO-np were 0.0042 ± 0.5 and 0.0025 ± 0.4, respectively, indicating a synergistic therapeutic interaction.

DISCUSSION

C. albicans is a major agent of hospital-acquired infections and the most prevalent systemic fungal pathogen in humans. Candidemia has been reported to be the fourth most common bloodstream infection of hospitalized patients in developed countries (4, 5), with *C. albicans* being highly related to catheter infections (3). In this study, we used *in vitro* assays and a well-described CVC model (22, 26) to mimic device-associated infection and to assess whether a sustained-released NO nanotechnology would prevent *C. albicans* biofilm formation. CVCs are major source of bloodstream infections in intensive care units (29), resulting in hospi-

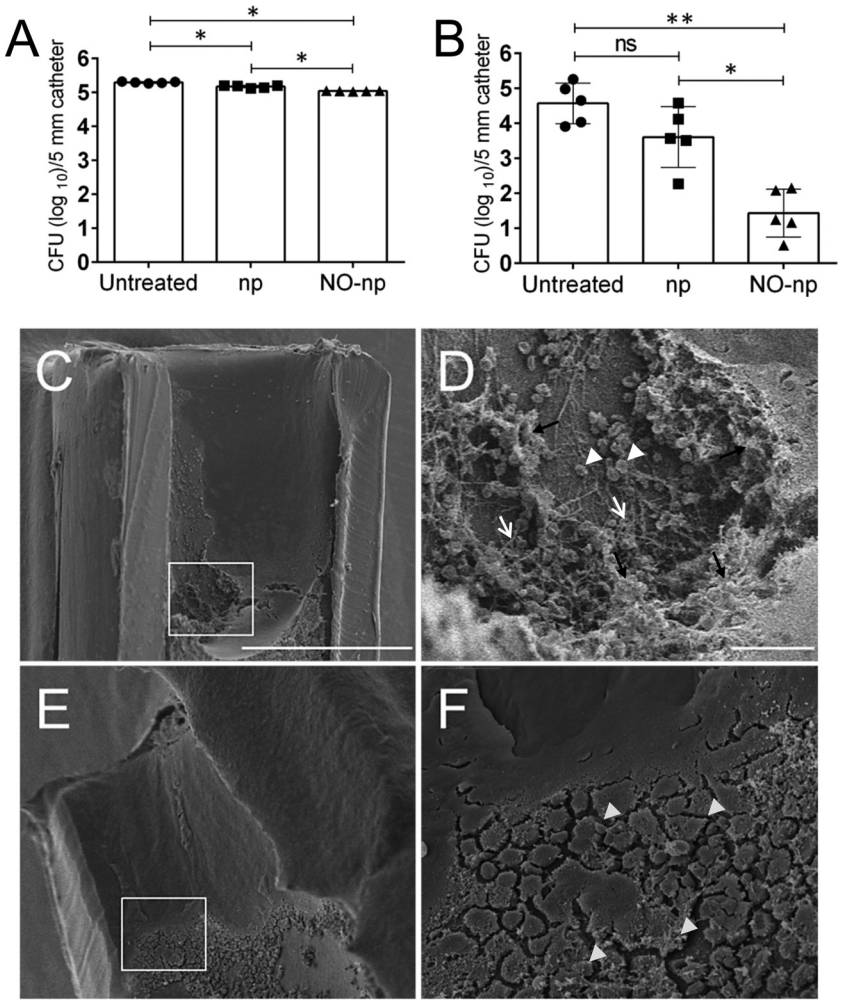

FIG 4 Reduction of *C. albicans* SC5314 surface-associated growth on central venous catheters (CVCs) inserted into rats' jugular veins after treatment with NO-np. Mean fungal burdens in *in vitro* (A) and *in vivo* (B) catheters infected with 10^6 *C. albicans* cells are shown. The fungal burden in NO-np-treated catheters was significantly lower than that in control catheters. For panel A, each symbol represents 5-mm catheters and the bars show the averages of five catheters. *In vitro* experiments were performed twice, with similar results obtained each time. For panel B, *in vivo* experiment was performed once using five animals (average of five 5-mm pieces of catheter per rat) per group. For panels A and B, a concentration of 5 mg/ml of np or NO-np was used. In addition, statistical significance (*, $P < 0.05$; **, $P < 0.001$; ns, no significance) was calculated using ANOVA and adjusted by use of the Bonferroni correction. Error bars indicate SDs. (C to F) *C. albicans* SC5314 strain biofilm formation on catheters placed on the jugular vein of a Sprague-Dawley rat. (C and D) Scanning electron microscopic (SEM) examination of untreated (PBS) *C. albicans* biofilms; (E and F) SEM examination of *C. albicans* biofilms treated with 5 mg/ml of NO-np. (C) *C. albicans* biofilm formed on the luminal surface of the untreated catheter. (D) Higher magnification of the boxed region in panel C. Untreated biofilms showed a network comprising yeast cells (white arrowheads) and hyphae (white arrows) surrounded by large amounts of exopolymeric matrix (black arrows). (E) There was no visible candidal biofilm formation in NO-np-treated catheters. (F) Higher magnification of the boxed region in panel E, with light gray arrowheads indicating fibrous debris. Scale bar for panels C and E, 200 μm; scale bar for panels D and F, 20 μm.

TABLE 1 Susceptibility of biofilm-associated *C. albicans* cells from clinical isolates to antimicrobials

Antimicrobial	50% RMA (μg/ml)[a]	50% RS (μg/ml)[b]
Voriconazole	64	32
Fluconazole	64	64
NO-np	5,000 (5.64×10^{-6}[c]; 3.76×10^{-6}[d,e])	5,000 (5.64×10^{-6}[c]; 3.76×10^{-6}[d,e])

[a] 50% RMA, a 50% reduction in metabolic activity, as determined by the XTT reduction assay.
[b] 50% RS, a 50% reduction in survival, as determined by the CFU killing assay.
[c] Actual nitric oxide in solution for initial peak.
[d] Actual nitric oxide in solution for steady state.
[e] $P < 0.05$.

talizations that last 1 to 2 weeks longer than otherwise warranted (30). Our results demonstrated that catheters treated with NO-np have reduced *C. albicans* biofilm formation *in vivo*. As expected, in the majority of the experiments, the control nanoparticle vehicle demonstrated less antibiofilm activity against *C. albicans* than NO-np.

We found that NO-np prevents biofilm formation and effectively kills yeasts and hyphae within mature biofilms. We have previously shown that NO-np interferes with fungal growth and morphogenesis during infection (18). The effects of the NO-np on fungal cells are potentially multifactorial, interfering with adhesion (31), colonization (32), and dissemination (33). Using annexin V-FITC and PI double staining, our studies revealed that

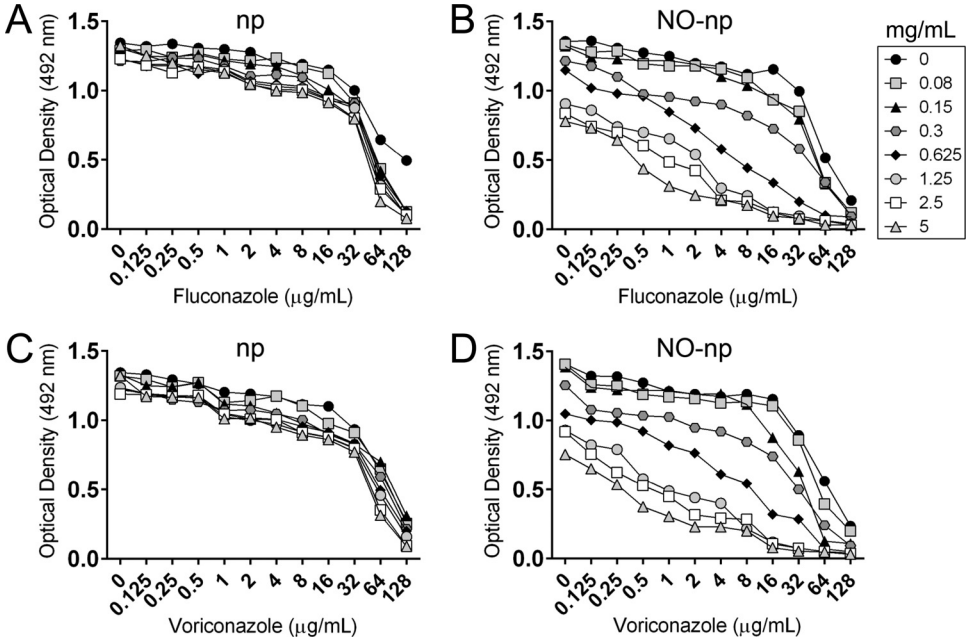

FIG 5 Combination therapy of nitric oxide and antifungal drugs reduces the metabolic activity of *C. albicans* SC5314 biofilms. Fungal biofilms were exposed to various combinations of np with fluconazole (A) or voriconazole (C) and NO-np with fluconazole (B) or voriconazole (D). The symbol key shows the concentration of np or NO-np tested alone or in combination with the antifungal drugs. The experiment was performed twice, with similar results obtained each time.

NO-np similarly promotes apoptosis and necrosis in fungal cell within biofilms. Annexin V-FITC and PI labeling visualization in *C. albicans* suggests that there is a more fundamental connection between the accumulation of NO and phosphatidylserine exposure as an event typical of apoptosis. In higher eukaryotes, cells that die due to necrosis do not follow the apoptotic signal transduction pathway, but rather, purinergic receptors are activated that result in the loss of cell membrane integrity and an uncontrolled release of products of cell death into the extracellular space (34). Although purinergic receptors have not been identified in *C. albicans*, evidence suggests that a similar necrotic activation pathway exists in fungi (35, 36).

One of the challenges, however, is to deliver NO gas constantly and steadily, and for its ultimate application, within a human body or prosthetic devices. Over the past several decades, countless research has been conducted to develop effective NO-generating and releasing materials for clinical therapies in response to the continuous discoveries pertaining to NO's importance in physiology and pathophysiology. A great number of synthetic compounds (e.g., *N*-diazeniumdiolates [37], nitrosothiols [38], and nitrosyl metal complexes [39]) have been developed to chemically stabilize and release NO in a controlled manner and have been exploited in many biomedical applications. However, the translation of the therapeutic potential of NO to the bedside has been limited by its short biological lifetime, instability during storage, and potential toxicity associated with many of these platforms (40). The NO-np platform is unique in that it does not rely on a donor molecule or even exogenous reduction of nitrite to NO, as observed with the clinically available organic nitrites and nitrates (e.g., nitroglycerin). Instead, the platform facilitates the reduction of encapsulated nitrite salt to NO through a stable dinitrogen trioxide intermediate, which, upon exposure to water, generates NO. Therefore, NO-np are rather true NO generators instead of donors like many of the aforementioned chemical entities (41). Additionally, we have demonstrated *in vitro* that NO-np show minimal toxicity toward cultured human lung fibroblasts (23). Furthermore, in *in vivo* safety (murine) evaluations using intraperitoneal and intravenous administration routes, minimal cytotoxicity was found, with no clinical adverse events occurring in the treated mice (42).

Our results show that a combination of NO-np and azole drugs has a synergistic effect against established fungal biofilms; in contrast, the combination of np and antifungals was not effective in eradicating *C. albicans* biofilms, highlighting the activity of the NO generated, not just the presence of nanoscopic materials. This phenomenon might be attributed to any of a number of the documented effects of NO. For example, reactivity of NO and its multiple redox states may cause inactivation of a variety of cellular enzymes, including ribonucleotide reductase, aconitase, and ubiquinone reductase (14, 43, 44). Similarly, NO has been reported to disrupt respiration, alter protein function, or cause lipid peroxidation and oxidation of sulfhydryl groups (14, 44). NO may also interact with DNA after penetration into the nuclei of microorganisms, resulting in deamination or cross-linking (14, 45), inhibition of mRNA synthesis, and interference with the synthesis of proteins. Our report showed the synergistic effects when NO-np and drug therapy are combined for treatment of those clinical situations (e.g., infected prosthetic devices) where the presence of established biofilms can be expected. One can anticipate that NO, a gas to which microbes develop minimal resistance even following repeated exposures (46), may contribute to the efficacy of drugs to which microorganisms within biofilms have resistance.

In conclusion, we demonstrated that NO-np have antimicrobial activity against *C. albicans* cells within biofilms. NO-np killed

yeast and hyphal forms of *C. albicans* cells by inducing apoptosis and causing necrosis, predominantly due to the multifactorial effects of the nanoparticle components on fungal cells. The roles of the apoptotic or necrotic pathway induced by NO should be further investigated. *C. albicans* biofilms were found to be even more susceptible to the combination of NO-np and azole drugs. Since catheter-related infections are difficult to treat and require constant removal of the devices, one can imagine situations where it may be possible to treat *C. albicans* biofilm-infected catheters *in situ* by local administration of NO-np alone or in combination with antifungal drugs (47); alternatively, as NO-np alone or in combination with antifungal drugs may have a role in preventing biofilm formation, a prophylactic dose may be administered immediately after insertion of the device or incorporated into the catheter material (48). Additionally, this nanotechnology is a flexible platform to encapsulate antimicrobial drugs for local delivery into infected catheters in order to prevent biofilm formation or eradicate mature biofilms (49). Together, these findings underscore the clear translational potential for the utilization of NO-np in the prevention and treatment of biofilms infecting medical prosthetic devices.

ACKNOWLEDGMENTS

M.S.A., H.H.L., D.A.S., M.T.T, K.P.D., and L.R.M. declare no conflict of interest. A.J.F. is a coinventor of the NO-np platform. A.J.F. and J.D.N. serve as advisors for the company Nano BioMed, Inc.

All authors contributed to the design of the experiments, analysis of the data, and writing of the manuscript. M.S.A. performed the *in vitro* biofilm formation and antimicrobial studies. A.J.F. synthesized control and NO-nanoparticles. J.D.N. provided the *C. albicans* clinical isolates. M.T.T., K.P.D., and L.R.M. collaborated in CVC biofilm model. D.A.S. performed SEM. H.H.L. performed the fluorescent microscopy and flow cytometry.

FUNDING INFORMATION

NYIT COM Start-up funds provided funding to Luis R Martinez. Valeant North America provided funding to Adam J Friedman.

REFERENCES

1. **Chandra J, Kuhn DM, Mukherjee PK, Hoyer LL, McCormick T, Ghannoum MA.** 2001. Biofilm formation by the fungal pathogen Candida albicans: development, architecture, and drug resistance. J Bacteriol **183:**5385–5394. http://dx.doi.org/10.1128/JB.183.18.5385-5394.2001.
2. **Donlan RM.** 2001. Biofilms and device-associated infections. Emerg Infect Dis **7:**277–281. http://dx.doi.org/10.3201/eid0702.010226.
3. **Kuhn DM, Ghannoum MA.** 2004. Candida biofilms: antifungal resistance and emerging therapeutic options. Curr Opin Investig Drugs **5:**186–197.
4. **Pappas PG, Rex JH, Sobel JD, Filler SG, Dismukes WE, Walsh TJ, Edwards JE, Infectious Diseases Society of America.** 2004. Guidelines for treatment of candidiasis. Clin Infect Dis **38:**161–189. http://dx.doi.org/10.1086/380796.
5. **Lamagni TL, Evans BG, Shigematsu M, Johnson EM.** 2001. Emerging trends in the epidemiology of invasive mycoses in England and Wales (1990-9). Epidemiol Infect **126:**397–414.
6. **Nguyen MH, Peacock JE, Jr, Tanner DC, Morris AJ, Nguyen ML, Snydman DR, Wagener MM, Yu VL.** 1995. Therapeutic approaches in patients with candidemia. Evaluation in a multicenter, prospective, observational study. Arch Intern Med **155:**2429–2435.
7. **Wilson LS, Reyes CM, Stolpman M, Speckman J, Allen K, Beney J.** 2002. The direct cost and incidence of systemic fungal infections. Value Health **5:**26–34. http://dx.doi.org/10.1046/j.1524-4733.2002.51108.x.
8. **Rello J, Ochagavia A, Sabanes E, Roque M, Mariscal D, Reynaga E, Valles J.** 2000. Evaluation of outcome of intravenous catheter-related infections in critically ill patients. Am J Respir Crit Care Med **162:**1027–1030. http://dx.doi.org/10.1164/ajrccm.162.3.9911093.
9. **Soufir L, Timsit JF, Mahe C, Carlet J, Regnier B, Chevret S.** 1999. Attributable morbidity and mortality of catheter-related septicemia in critically ill patients: a matched, risk-adjusted, cohort study. Infect Control Hosp Epidemiol **20:**396–401. http://dx.doi.org/10.1086/501639.
10. **Uppuluri P, Chaturvedi AK, Srinivasan A, Banerjee M, Ramasubramaniam AK, Kohler JR, Kadosh D, Lopez-Ribot JL.** 2010. Dispersion as an important step in the Candida albicans biofilm developmental cycle. PLoS Pathog **6:**e1000828. http://dx.doi.org/10.1371/journal.ppat.1000828.
11. **LaFleur MD, Kumamoto CA, Lewis K.** 2006. Candida albicans biofilms produce antifungal-tolerant persister cells. Antimicrob Agents Chemother **50:**3839–3846. http://dx.doi.org/10.1128/AAC.00684-06.
12. **Fauvart M, De Groote VN, Michiels J.** 2011. Role of persister cells in chronic infections: clinical relevance and perspectives on anti-persister therapies. J Med Microbiol **60:**699–709. http://dx.doi.org/10.1099/jmm.0.030932-0.
13. **Bink A, Vandenbosch D, Coenye T, Nelis H, Cammue BP, Thevissen K.** 2011. Superoxide dismutases are involved in Candida albicans biofilm persistence against miconazole. Antimicrob Agents Chemother **55:**4033–4037. http://dx.doi.org/10.1128/AAC.00280-11.
14. **De Groote MA, Fang FC.** 1995. NO inhibitions: antimicrobial properties of nitric oxide. Clin Infect Dis **21**(Suppl 2)**:**S162–S165.
15. **Vazquez-Torres A, Jones-Carson J, Balish E.** 1995. Nitric oxide production does not directly increase macrophage candidacidal activity. Infect Immun **63:**1142–1144.
16. **Jones-Carson J, Vazquez-Torres A, van der Heyde HC, Warner T, Wagner RD, Balish E.** 1995. Gamma delta T cell-induced nitric oxide production enhances resistance to mucosal candidiasis. Nat Med **1:**552–557. http://dx.doi.org/10.1038/nm0695-552.
17. **Ghaffari A, Miller CC, McMullin B, Ghahary A.** 2006. Potential application of gaseous nitric oxide as a topical antimicrobial agent. Nitric Oxide **14:**21–29. http://dx.doi.org/10.1016/j.niox.2005.08.003.
18. **Macherla C, Sanchez DA, Ahmadi MS, Vellozzi EM, Friedman AJ, Nosanchuk JD, Martinez LR.** 2012. Nitric oxide releasing nanoparticles for treatment of Candida albicans burn infections. Front Microbiol **3:**193. http://dx.doi.org/10.3389/fmicb.2012.00193.
19. **Tillmann A, Gow NA, Brown AJ.** 2011. Nitric oxide and nitrosative stress tolerance in yeast. Biochem Soc Trans **39:**219–223. http://dx.doi.org/10.1042/BST0390219.
20. **Martinez LR, Han G, Chacko M, Mihu MR, Jacobson M, Gialanella P, Friedman AJ, Nosanchuk JD, Friedman JM.** 2009. Antimicrobial and healing efficacy of sustained release nitric oxide nanoparticles against Staphylococcus aureus skin infection. J Invest Dermatol **129:**2463–2469. http://dx.doi.org/10.1038/jid.2009.95.
21. **Han G, Martinez LR, Mihu MR, Friedman AJ, Friedman JM, Nosanchuk JD.** 2009. Nitric oxide releasing nanoparticles are therapeutic for Staphylococcus aureus abscesses in a murine model of infection. PLoS One **4:**e7804. http://dx.doi.org/10.1371/journal.pone.0007804.
22. **Andes D, Nett J, Oschel P, Albrecht R, Marchillo K, Pitula A.** 2004. Development and characterization of an in vivo central venous catheter Candida albicans biofilm model. Infect Immun **72:**6023–6031. http://dx.doi.org/10.1128/IAI.72.10.6023-6031.2004.
23. **Friedman AJ, Han G, Navati MS, Chacko M, Gunther L, Alfieri A, Friedman JM.** 2008. Sustained release nitric oxide releasing nanoparticles: characterization of a novel delivery platform based on nitrite containing hydrogel/glass composites. Nitric Oxide **19:**12–20. http://dx.doi.org/10.1016/j.niox.2008.04.003.
24. **Zhang X, Broderick M.** 2000. Amperometric detection of nitric oxide. Mod Aspects Immunobiol **1:**160–165.
25. **Meshulam T, Levitz SM, Christin L, Diamond RD.** 1995. A simplified new assay for assessment of fungal cell damage with the tetrazolium dye, (2,3)-bis-(2-methoxy-4-nitro-5-sulphenyl)-(2H)-tetrazolium-5-carboxanil ide (XTT). J Infect Dis **172:**1153–1156. http://dx.doi.org/10.1093/infdis/172.4.1153.
26. **Martinez LR, Mihu MR, Tar M, Cordero RJ, Han G, Friedman AJ, Friedman JM, Nosanchuk JD.** 2010. Demonstration of antibiofilm and antifungal efficacy of chitosan against candidal biofilms, using an in vivo central venous catheter model. J Infect Dis **201:**1436–1440. http://dx.doi.org/10.1086/651558.
27. **Martinez LR, Casadevall A.** 2006. Susceptibility of Cryptococcus neoformans biofilms to antifungal agents in vitro. Antimicrob Agents Chemother **50:**1021–1033. http://dx.doi.org/10.1128/AAC.50.3.1021-1033.2006.
28. **Chandra J, Mukherjee PK, Leidich SD, Faddoul FF, Hoyer LL, Douglas**

LJ, Ghannoum MA. 2001. Antifungal resistance of candidal biofilms formed on denture acrylic in vitro. J Dent Res **80:**903–908. http://dx.doi.org/10.1177/00220345010800031101.
29. **Richards MJ, Edwards JR, Culver DH, Gaynes RP.** 1999. Nosocomial infections in medical intensive care units in the United States. National Nosocomial Infections Surveillance System. Crit Care Med **27:**887–892.
30. **Pittet D, Tarara D, Wenzel RP.** 1994. Nosocomial bloodstream infection in critically ill patients. Excess length of stay, extra costs, and attributable mortality. JAMA **271:**1598–1601.
31. **Privett BJ, Nutz ST, Schoenfisch MH.** 2010. Efficacy of surface-generated nitric oxide against Candida albicans adhesion and biofilm formation. Biofouling **26:**973–983. http://dx.doi.org/10.1080/08927014.2010.534552.
32. **Elahi S, Pang G, Ashman RB, Clancy R.** 2001. Nitric oxide-enhanced resistance to oral candidiasis. Immunology **104:**447–454. http://dx.doi.org/10.1046/j.1365-2567.2001.01331.x.
33. **Glittenberg MT, Kounatidis I, Christensen D, Kostov M, Kimber S, Roberts I, Ligoxygakis P.** 2011. Pathogen and host factors are needed to provoke a systemic host response to gastrointestinal infection of Drosophila larvae by Candida albicans. Dis Model Mech **4:**515–525. http://dx.doi.org/10.1242/dmm.006627.
34. **Proskuryakov SY, Konoplyannikov AG, Gabai VL.** 2003. Necrosis: a specific form of programmed cell death? Exp Cell Res **283:**1–16. http://dx.doi.org/10.1016/S0014-4827(02)00027-7.
35. **Koshlukova SE, Lloyd TL, Araujo MW, Edgerton M.** 1999. Salivary histatin 5 induces non-lytic release of ATP from Candida albicans leading to cell death. J Biol Chem **274:**18872–18879. http://dx.doi.org/10.1074/jbc.274.27.18872.
36. **Vylkova S, Sun JN, Edgerton M.** 2007. The role of released ATP in killing Candida albicans and other extracellular microbial pathogens by cationic peptides. Purinergic Signal **3:**91–97. http://dx.doi.org/10.1007/s11302-006-9040-0.
37. **Duong HT, Jung K, Kutty SK, Agustina S, Adnan NN, Basuki JS, Kumar N, Davis TP, Barraud N, Boyer C.** 2014. Nanoparticle (star polymer) delivery of nitric oxide effectively negates Pseudomonas aeruginosa biofilm formation. Biomacromolecules **15:**2583–2589. http://dx.doi.org/10.1021/bm500422v.
38. **Kishikawa H, Ebberyd A, Romling U, Brauner A, Luthje P, Lundberg JO, Weitzberg E.** 2013. Control of pathogen growth and biofilm formation using a urinary catheter that releases antimicrobial nitrogen oxides. Free Radic Biol Med **65:**1257–1264. http://dx.doi.org/10.1016/j.freeradbiomed.2013.09.012.
39. **Halpenny GM, Gandhi KR, Mascharak PK.** 2010. Eradication of pathogenic bacteria by remote delivery of nitric oxide via light-triggering of nitrosyl-containing materials. ACS Med Chem Lett **1:**180–183. http://dx.doi.org/10.1021/ml1000646.
40. **Friedman A, Friedman J.** 2009. New biomaterials for the sustained release of nitric oxide: past, present and future. Expert Opin Drug Deliv **6:**1113–1122. http://dx.doi.org/10.1517/17425240903196743.
41. **Kutner AJ, Friedman AJ.** 2013. Use of nitric oxide nanoparticulate platform for the treatment of skin and soft tissue infections. Wiley Interdiscip Rev Nanomed Nanobiotechnol **5:**502–514.
42. **Cabrales P, Han G, Nacharaju P, Friedman AJ, Friedman JM.** 2011. Reversal of hemoglobin-induced vasoconstriction with sustained release of nitric oxide. Am J Physiol Heart Circ Physiol **300:**H49–H56. http://dx.doi.org/10.1152/ajpheart.00665.2010.
43. **Drapier JC, Hibbs JB, Jr.** 1996. Aconitases: a class of metalloproteins highly sensitive to nitric oxide synthesis. Methods Enzymol **269:**26–36. http://dx.doi.org/10.1016/S0076-6879(96)69006-5.
44. **Farias-Eisner R, Chaudhuri G, Aeberhard E, Fukuto JM.** 1996. The chemistry and tumoricidal activity of nitric oxide/hydrogen peroxide and the implications to cell resistance/susceptibility. J Biol Chem **271:**6144–6151. http://dx.doi.org/10.1074/jbc.271.11.6144.
45. **Tamir S, DeRojas-Walker T, Wishnok JS, Tannenbaum SR.** 1996. DNA damage and genotoxicity by nitric oxide. Methods Enzymol **269:**230–243. http://dx.doi.org/10.1016/S0076-6879(96)69025-9.
46. **Privett BJ, Broadnax AD, Bauman SJ, Riccio DA, Schoenfisch MH.** 2012. Examination of bacterial resistance to exogenous nitric oxide. Nitric Oxide **26:**169–173. http://dx.doi.org/10.1016/j.niox.2012.02.002.
47. **Guzman LA, Labhasetwar V, Song C, Jang Y, Lincoff AM, Levy R, Topol EJ.** 1996. Local intraluminal infusion of biodegradable polymeric nanoparticles. A novel approach for prolonged drug delivery after balloon angioplasty. Circulation **94:**1441–1448.
48. **Evliyaoglu Y, Kobaner M, Celebi H, Yelsel K, Dogan A.** 2011. The efficacy of a novel antibacterial hydroxyapatite nanoparticle-coated indwelling urinary catheter in preventing biofilm formation and catheter-associated urinary tract infection in rabbits. Urol Res **39:**443–449. http://dx.doi.org/10.1007/s00240-011-0379-5.
49. **Sanchez DA, Schairer D, Tuckman-Vernon C, Chouake J, Kutner A, Makdisi J, Friedman JM, Nosanchuk JD, Friedman AJ.** 2014. Amphotericin B releasing nanoparticle topical treatment of Candida spp. in the setting of a burn wound. Nanomedicine **10:**269–277. http://dx.doi.org/10.1016/j.nano.2013.06.002.